while, correspondingly for neutral dipions [reaction (2)],

$$x=\tfrac{1}{9}[\sin^2\delta_2+4\sin^2\delta_0+4\sin\delta_0\sin\delta_2\cos(\delta_0-\delta_2)]+9(d_{00}{}^1)^2\sin^2\delta_1,$$
$$y=2d_{00}{}^1[\sin\delta_2\sin\delta_1\cos(\delta_0-\delta_1)+2\sin\delta_0\sin\delta_1\times\cos(\delta_2-\delta_1)]. \quad (21)$$

Referring back to Eqs. (10) and (11) and recalling the nature of the data, we see that both x and y are extrapolations of large moments in the cross section for reaction (2) and can be accurately determined with the statistics of experiments now underway. The extrapolated moment z- and the φ-dependent terms will be difficult to determine but can, in principle, be determined and serve as a test of the procedure. Using just x and y for reaction (2), we see there are two equations and three unknowns. With both charged and neutral dipion experiments, using just these two moments, all three phase shifts can be determined.

CONCLUSIONS

Extrapolation in $\pi N\rightarrow\pi\pi N$ is a hopeful technique for extracting the $\pi\pi$ amplitude in the ρ region and below. Very low $-t$ ($\lesssim 4\mu^2$) should be investigated. Experiments in the 5–10-GeV/c region look most promising. Rapid t dependences can be hoped to be absent in certain moments. Interesting results will be obtained, extrapolating two moments with a few thousand events. It would be nice if other moments could be handled to check the procedure. Of course, reasonable behavior of δ_1 is an important check. The moment analysis can be carried out in both G-J and H frames as a check. The behavior in the two frames is rather different, but theoretical models do not make it clear that one frame is more promising than the other for extrapolation.

ACKNOWLEDGMENTS

We would like to thank Dr. I Dorado and Professor W. Selove for useful discussion.

PHYSICAL REVIEW VOLUME 177, NUMBER 5 25 JANUARY 1969

Diffraction Dissociation and the Production of Baryon Resonances

J. G. RUSHBROOKE
Cavendish Laboratory, University of Cambridge, Cambridge, England
(Received 10 June 1968; revised manuscript received 17 October 1968)

A model incorporating virtual-meson diffraction scattering followed by a final-state resonant interaction of the meson with an emergent nucleon or isobar is proposed for the production of $I=\frac{1}{2}$ baryon resonances in the reaction $pp\rightarrow pN_{1/2}{}^*$. Absolute predictions are compared with the experimental data relating to enhancements observed in missing-mass experiments. Agreement is favorable in the case of the $P_{11}(1470)$, but otherwise the many resonances predicted by phase-shift analyses complicate the issue and prevent a clear-cut test of the model. The proposed $\Delta P=(-1)^{\Delta J}$ selection rule is discussed in relation to the large cross section predicted by the model for the "forbidden" $S_{11}(1550)$.

I. INTRODUCTION

EXPERIMENTAL studies[1–5] of the reaction $pp\rightarrow pN^*$ at high energies have recently attracted considerable interest as possible examples of the reaction mechanism known as diffraction dissociation,[6] which is thought to possess the following characteristic features:

1. Constant total cross section at high energies.
2. A very low momentum-transfer elastic scattering between the incident particles leads to the materialization of the dissociated system. The dissociation products (in this case the decay products of the N^*) therefore have a diffractive distribution.
3. The larger the mass change in the dissociation process the less the probability and the higher the energy required.
4. Zero transfer of quantum numbers such as B, Q, S, I, G, C in the process, which is sometimes visualized[7] as "vacuon" or "Pomeranchukon" exchange.
5. Only orbital angular momentum (not internal-symmetry quantum numbers) may be transferred to the dissociating system. Thus only "natural parity" changes are allowed, $\Delta P=(-1)^{\Delta L}$. With incident pseudoscalar particles, the transition $0^-\rightarrow 0^-$, 1^+, $2^-\cdots$, can occur, but not $0^-\rightarrow 0^+$, 1^-, 2^+, $3^-\cdots$. With incident baryons no final states are disallowed, and a stronger rule $\Delta P=(-1)^{\Delta J}$ has been suggested,[8] requiring $\frac{1}{2}^+\rightarrow\frac{1}{2}^+$, $\frac{3}{2}^-$, $\frac{5}{2}^+$, $\frac{7}{2}^-$, $\cdots$, only. However, the experimental evidence concerning this rule is inconclusive, and it has

[1] G. Belletini *et al.*, Phys. Letters **18**, 167 (1967).
[2] E. W. Anderson *et al.*, Phys. Rev. Letters **16**, 855 (1966).
[3] I. M. Blair *et al.*, Phys. Rev. Letters **17**, 789 (1966).
[4] K. J. Foley *et al.*, Phys. Rev. Letters **19**, 397 (1967).
[5] H. L. Anderson *et al.*, Phys. Rev. Letters **18**, 90 (1967).
[6] M. L. Good and W. D. Walker, Phys. Rev. **120**, 1857 (1960).
[7] M. Ross and L. Stodolsky, Phys. Rev. **149**, 1172 (1966).
[8] D. R. O. Morrison, Phys. Rev. **165**, 1699 (1968).

as yet no theoretical basis. We refer to these baryon states as having natural parity.

The first property implies that the process will probably dominate at high energies. Morrison[9] has shown that the cross sections for two-body and quasi-two-body reactions may be expressed phenomenologically in terms of the incident laboratory momentum p_{inc} in the form

$$\sigma = \text{const}\ p_{\text{inc}}^{-n},$$

where the exponent n is to be determined from data at high energy ($\gtrsim 2$ GeV/c). Anderson *et al.*[2] found almost constant cross sections ($n \approx 0.2$) in the range 10–30 BeV/c for the production of enhancements which were taken to be the 1400-, 1520-, 1690-, and 2190-MeV sequence of $N_{1/2}^*$ isobars which have $J = \frac{1}{2}^+, \frac{3}{2}^-, (\frac{5}{2})^\pm$, and $\frac{7}{2}^-$ and so qualify as natural parity states. In contrast, a steeply falling cross section was found for the 1236-MeV $N_{3/2}^*$ isobar, which requires $I=1$ exchange and so cannot be produced by diffraction dissociation. The slope b in a fit of the form

$$d\sigma/dt = Ae^{-b|t|},$$

to the differential cross sections with respect to 4-momentum transfer t was found to vary from $\sim$15–20 (BeV/c)$^{-2}$ for the 1400-MeV isobar to 4–5 (BeV/c)$^{-2}$ for the higher isobars.

In a Regge-pole theory, $d\sigma/dt$ is proportional to $s^{2\alpha(t)-2}$ and as most of the two-body cross sections are concentrated near $t=0$, and at high energies $p_{\text{inc}} \propto s$, this gives $n \approx |2\alpha(0)-2|$. The near-zero value of n is therefore in accord with what one might expect from

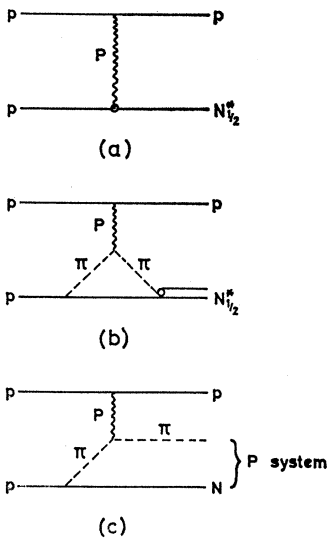

FIG. 1. (a) Diagram for $pp \to pN_{1/2}^*$ by "inelastic Pomeranchukon" exchange, where $N_{1/2}^*$ is a "natural parity" nucleon resonance. (b) Diagram for $pp \to pN_{1/2}^*$ by "elastic Pomeranchukon" exchange, evocative of the diffraction dissociation process with recombination. (c) Drell-Hiida process.

[9] D. R. O. Morrison, Phys. Letters **22**, 528 (1966).

"vacuon" or "Pomeranchukon" exchange, for which $\alpha(0)=1$ is assumed. The most general diagram for this process would be that of Fig. 1(a), which Morrison[8] calls "inelastic Pomeranchukon" exchange. A particular case [Fig. 1(b)] of this diagram he calls "elastic Pomeranchukon" exchange, in which the dissociation $p \to N+\pi$ of one proton is followed by diffraction scattering of the virtual pion off the other proton and then by recombination of the pion with a baryon to produce an $N_{1/2}^*$.

It was pointed out a long time ago by Drell and Hiida[10] that even without the recombination or any final-state interaction, a low-mass bump of the pion-baryon system will result from the process as a purely kinematic effect at sufficiently high energies, and the $N^*(1400)$ has recently received special attention[11] from this point of view. This is equivalent to using the diagram of Fig. 1(c). The idea has also gained currency with meson-baryon interactions in trying to understand the $A_1(\pi\rho)$ bump in $\pi p \to \pi\rho N$ (the so-called "Deck effect") and to shed light on the low-energy structure in the $K\pi\pi$ system produced in $KN \to K^*\pi N$. Various calculations[11–15] have sought to account for the position, width, production cross section, and behavior as a function of beam energy of these bumps with varying degrees of success. The general question of kinematic backgrounds has now assumed great importance in trying to identify "genuine" resonances, since background-amplitude and resonance-producing amplitudes could interfere, sometimes with very confusing results.[16] The major properties of such backgrounds appear well established theoretically; for example, there is the interesting result[14] that the scattering of a heavier virtual particle appears to be just as important as that of a lighter one [e.g., a ρ instead of a π in Fig. 1(c)]. Also "helicity conservation" at the dissociation vertex, because of vacuon exchange, means a Treiman-Yang-type isotropy test about the beam direction when it is an incident meson which dissociates; such behavior has been observed[14] in the case of the A_1. More recently, Chew and Pignotti[17] have pointed out that resonances are already contained to some degree in these background amplitudes in some average sense, and a Deck peak amounts therefore to a prediction of a low-mass resonance or resonances. At this stage it is not clear how to estimate this contribution to resonance production and all cross-section estimates, whether experimental or theoretical, share this uncertainty over background.

In this paper we wish to explore a simple model based

[10] S. D. Drell and K. Hiida, Phys. Rev. Letters **7**, 199 (1961).
[11] L. Resnick, Phys. Rev. **150**, 1292 (1966).
[12] R. T. Deck, Phys. Rev. Letters **13**, 169 (1964).
[13] U. Maor and T. A. O'Halloran, Jr., Phys. Letters **15**, 281 (1965).
[14] L. Stodolsky, Phys. Rev. Letters **18**, 973 (1967).
[15] M. Ross and Y. Y. Yam, Phys. Rev. Letters **19**, 546 (1967). (A comprehensive list of references may be found here.)
[16] G. Goldhaber, Phys. Rev. Letters **19**, 976 (1967).
[17] G. F. Chew and A. Pignotti, Phys. Rev. Letters **20**, 1078 (1968).

on Fig. 1(b), but more general, with a view to predicting total cross sections and $d\sigma/dt$'s for $N_{1/2}$*'s. We start with amplitudes of the Drell-Hiida type [Fig. 1(c)], and resolve them into amplitudes connecting states of definite total angular momentum and parity of the dissociation products P. A final-state resonant interaction between scattered pion and emergent baryon is then introduced phenomenologically to represent the diagram of Fig. 1(b), and the cross section for production of a particular N^* obtained by integrating the cross section, considered as a function of the mass of the P system, under the N^*'s resonant peak. A model of this sort has been anticipated by Resnick[11] in considering production of the 1400 peak by diffraction dissociation. Our model is described in Sec. II.

We are thus turning aside from the diffraction dissociation process regarded purely as a background mechanism, and thinking of it as the dominant mechanism for the generation of bona-fide resonances.

The N^* production data of experimenters such as Anderson *et al.*[2] is based on experiments of the missing-mass spectrometer type, in which the mass of the system recoiling from an observed fast proton in the laboratory and the 4-momentum transfer to it were calculated from the momentum and scattering angle of the detected proton. The observed resonant bumps were always superimposed upon large background, which presumably comes from many competing processes, including diagrams of the Drell-Hiida type, and exchange diagrams where the observed proton is itself the decay product of a resonance. Examination of particular final states from pp interactions[18] in bubble-chamber experiments shows clear peaking in excess of the kinematic reflection of one-pion-exchange diagrams, which is evidently due to reaction channels like $pp \to N^*(1450)p \to p\pi^+\pi^- p$ and $pp \to N^*(1450)p \to n\pi^+ p$. Cross-section estimates for $pp \to N^*(1450)p$, allowing for unseen charge states, give values at least compatible with counter data. For the purposes of this calculation we shall therefore assume that the sharp peaks measured in missing-mass experiments correspond principally to diagrams like Fig. 1(b), containing a final-state resonant interaction. As Fig. 1(c) gives a relatively smooth mass distribution this contribution is assumed lost in the general missing-mass background, though in the Chew-Pignotti sense it does contain some genuine resonant amplitude. We shall return to this question at the end of Sec. IV.

Other attempts at explaining the reactions $pp \to pN_{1/2}$* have been made. Pion exchange fails to give[19] either the correct energy behavior or normalization. A surface-excitation droplet model succeeds quite well in giving[20] the energy independence of the total cross section and the correct slopes of $d\sigma/dt$ for the 1400- and 1520-MeV isobars but fails completely to predict the correct slopes for the 1690- and 2190-MeV isobars. An impact-parameter cutoff model predicts[21] all the slopes correctly but has many unknown parameters to adjust. Neither of these models gives absolute normalization and both predict a secondary maximum at $t=0.4$ GeV/c^2 for the 1400-MeV isobar which does not seem to be consistent with experimental data.

II. MODEL

A. Preliminaries

The diagram for the model is given in Fig. 2(a) and again in Fig. 2(b) after the inclusion of the final-state resonant interaction which generates N^*'s of spin J and parity $\mathcal{P}$. The particle p_2' is intended to be either a nucleon, as in the Drell-Hiida model, or a $\frac{3}{2}^+$ isobar [the $\Delta(1236)$]. Input channels for the final-state interaction have been considered only, if they are strongly coupled to the known $N_{1/2}$*'s. Referring to the data[22] on observed decay modes, one sees that the $N\pi$ and $N\pi\pi$ modes dominate, with some $\Delta(1236)\pi$ channel now fairly certain in several cases on the basis of latest evidence[23]; the model therefore allows for production of a Δ at the bottom vertex. Further evidence for a strong $N\pi\Delta$ vertex operating in pp interactions comes from experiment[18]—from 30–50% of certain final states (like $pn\pi^+$, $pp\pi^+\pi^-$) contain Δ^{++}'s. An $N\pi\pi$ (i.e., 3-body) system would appear to be an unlikely input channel for final-state N^* production, and lies outside the scope of

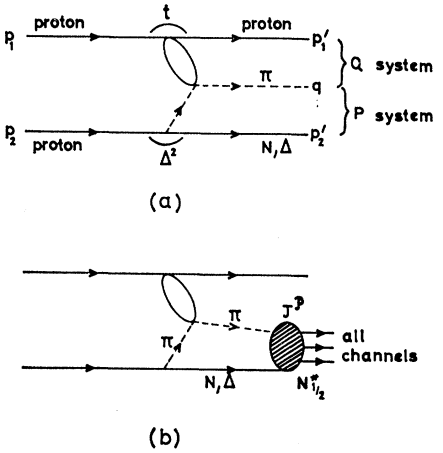

FIG. 2. (a) Diagram for $pp \to pN\pi$ and $pp \to p\Delta\pi$. For notation see text. (b) Same with inclusion of final-state resonance interaction $\pi(N \text{ or } \Delta) \to N_{1/2}$*.

[18] J. G. Rushbrooke, in Proceedings of the International Conference on High Energy Physics, Vienna, 1968 (to be published), contains a review of the experimental evidence.

[19] P. C. M. Yock, Nuovo Cimento **44**, 777 (1966); B. Margolis and A. Rotsstein, *ibid.* **45**, 1010 (1966); G. Alexander *et al.*, *ibid.* **40**, 839 (1965); B. Haber and G. Yekutieli, Phys. Rev. **160**, 1410 (1967).

[20] R. C. Arnold, Phys. Rev. **157**, 1292 (1967).

[21] A. Rotsstein, Nucl. Phys. **B1**, 655 (1967).

[22] N. Barash-Schmidt *et al.*, University of California Radiation Laboratory Report No. UCRL 8030-Pt.I (Rev.), 1968 (unpublished).

[23] A. Donnachie, in Proceedings of the International Conference on High Energy Physics, Vienna, 1968 (to be published).

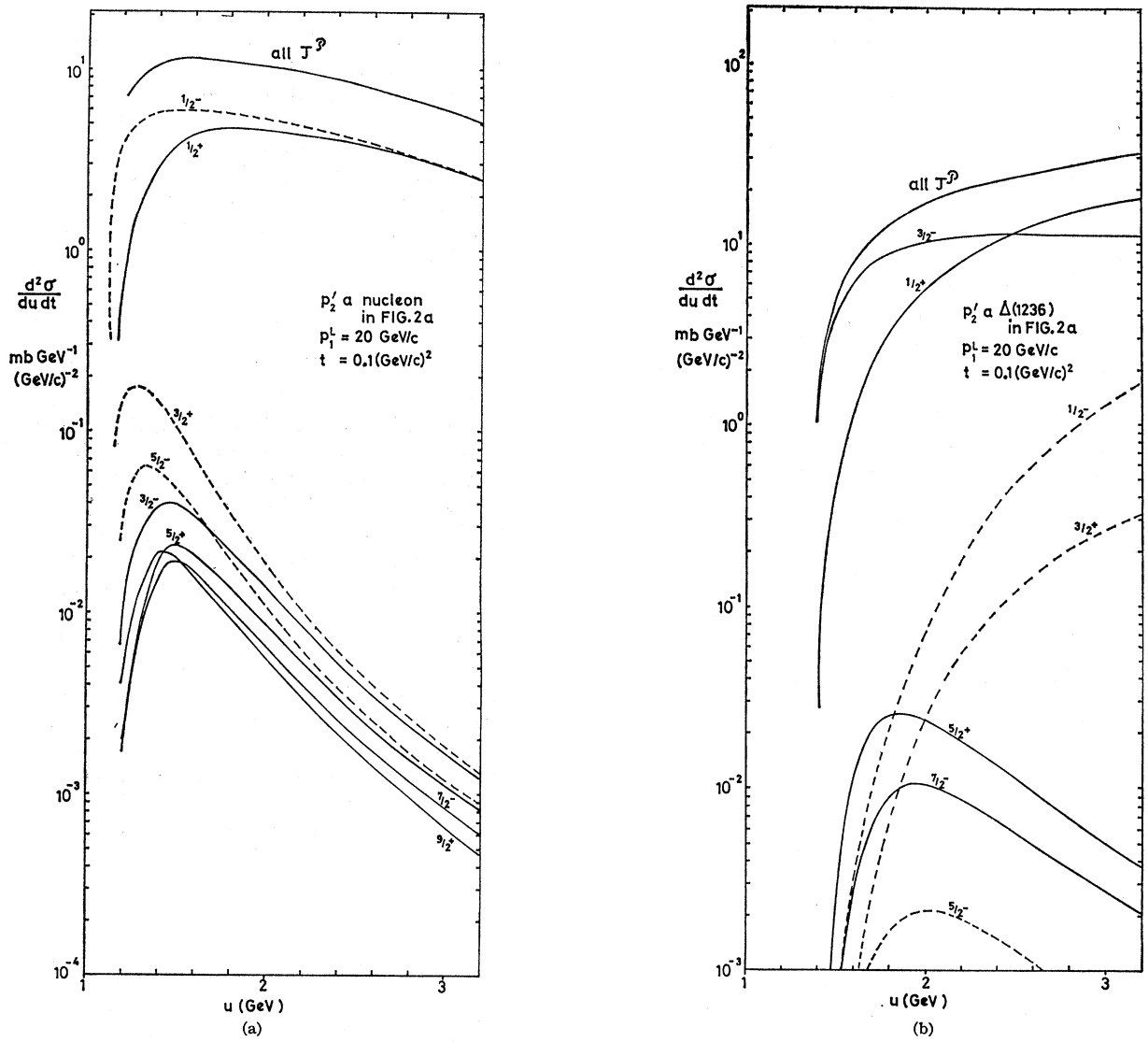

FIG. 3. (a) Differential cross section versus mass u of P system in various states $J^{\mathcal{P}}$ obtained from Eq. (10a) for diagram of Fig. 2(a) with p_2' a nucleon calculated at fixed $t=0.1$ (GeV/c)^2. Natural parity states are full curves, "unnatural" parity states are dashed curves. The curve labelled "all J" is calculated from Eq. (17). (b) Same for Fig. 3(a) with p_2' a $\Delta(1236)$.

this model. The $N\eta$ decay mode dominates and will be considered in the case of the $S_{11}(1550)$, but is very minor for other resonances. Strange-particle $(\Lambda/\Sigma K)$ modes and recently reported more exotic ones such as $\Delta\rho$, $\Delta\pi\pi$, and $Y^*(1385)K$ are also unimportant, and will therefore be neglected as intermediate states.

As we shall see, taking p_2' to be both a nucleon and a $\frac{3}{2}^+$ isobar means $J=\frac{1}{2}$ and $J=\frac{3}{2}$ states can be produced strongly, but higher-J states are suppressed [see Figs. 3(a) and 3(b)]. These higher-J states could be amplified if the model were extended to higher-spin p_2', but we exclude this possibility on grounds of nonobservation of the corresponding $N_J^* \to p_2'$ decay modes, though this is perhaps due more to decay phase-space limitations than smallness of decay matrix elements. However, uncertainties arising from the off-shell nature of intermediate-state particles remain, and a less crude final-state-interaction calculation is probably a more pressing refinement of the model. In any case, close examination of the experimental evidence does not show beyond doubt that higher-J ($\gtrsim\frac{5}{2}$) isobars [like the $F_{15}(1690)$ and $G_{17}(2190)$] are being observed, so the model may not necessarily be inadequate in this respect. This will be discussed further in Sec. III.

There are several other graphs which could possibly contribute but are neglected: (i) ρ scattering instead of π scattering at the top vertex; the same arguments as above may now be applied to $N^* \to N\rho$, $\Delta\rho$ decays; (ii) inelastic scattering of an object off the Pomeranchukon at the top vertex to produce a pion; this object

would have to have $I=1$, $G=-$, $J=0^-$, 1^+, 2^-, $\cdots$, and there is as yet no well-confirmed candidate (the A_1 is a possibility); (iii) scattering of the baryon instead of the pion at the top vertex, corresponding to the incident proton p_1 scattering off the core instead of the pion cloud of proton p_2; there is no evidence that baryon exchange contributes significantly in high-energy pp collisions to the intermediate states considered here; (iv) diffraction scattering at the bottom vertex instead of the top one; as p_1' is the fast proton detected in a missing-mass experiment, this diagram would only contribute to background (see Ref. 24).

Figure 2(a) will therefore be calculated on the assumption that p_2' is either a nucleon or $\frac{3}{2}^+$ $\Delta(1236)$ isobar, and all charge states of the P system will be summed over. As the cross sections for N^* production have been determined in a missing-mass experiment with only the recoil proton (p_1') observed, all decay channels of the N^* will be summed over by taking the full width of the appropriate N^* in the decay channel. $t=(p_1'-p_1)^2$ is the invariant momentum transfer squared at the diffraction vertex, and $\Delta^2=(p_2'-p_2)^2$ that at the dissociation vertex. The metric is defined so that t, $\Delta^2>0$. Other invariants needed are the invariant masses squared $W^2=-(p_1+p_2)^2$ of the whole system, $w^2=-(p_1'+q)^2$ of the diffracting system, and $u^2=-(q+p_2')^2$ of the resonating system; t and u are the quantities measured in missing-mass experiments. The masses of the incoming particles are m_1, m_2 and of the outgoing particles m_1', m, and m_2'. The diffracting system will be referred to as the Q system, and the resonating system as the P system; quantities evaluated in each rest frame will be superscripted accordingly. Similarly L refers to the laboratory frame, where $p_2{}^L=0$.

The kinematic framework has been well described[10–12] previously, and we refer the reader there for details. In the equations that follow, (a) refers to the case where p_2' is a $\frac{1}{2}^+$ baryon and (b) to where p_2' is a $\frac{3}{2}^+$ baryon.

The invariant amplitude before decomposing into P states of definite J and $\mathcal{P}$ may be written

$$M=M_1(w^2,t)(\Delta^2+\mu^2)^{-1}G\bar{u}(p_2')\gamma_5 u(p_2) \qquad (1a)$$

or

$$M=M_1(w^2,t)(\Delta^2+\mu^2)^{-1}(G^*/\mu)\bar{U}_\mu(p_2')u(p_2)p_{2\mu}, \qquad (1b)$$

where μ is the pion mass and the coupling constants have the values $G^2/4\pi=14.4$ and $G^{*2}/4\pi=0.37$. Spinors are normalized to $2m$. M_1 is the invariant amplitude for the $\pi N\to\pi N$ diffraction scattering process, and using the optical theorem in the customary manner one has

$$\frac{d\sigma}{d\Omega}(w^2,t)=\frac{1}{64w^2\pi^2}\sum\tfrac{1}{2}|M_1|^2=\frac{(q^Q)^2}{16\pi^2}\sigma_{\rm tot}{}^2(w)g(t), \qquad (2)$$

so that

$$\tfrac{1}{2}\sum|M_1|^2=4(q^Q)^2w^2\sigma_{\rm tot}{}^2(w)g(t), \qquad (3)$$

where $\sum$ means a sum over initial and final spin states and $\mathbf{q}^Q$ is of course the 3-momentum of scattering in the Q frame. We make the approximation $w^2(q^Q)^2\approx\frac{1}{4}(w^2-m_1{}'{}^2)^2$ since $m^2\ll m_1{}'{}^2$, and let $\sigma_{\rm tot}{}^2(w)$ tend to its observed asymptotic value independent of w.

The differential cross section for the whole process is

$$d\sigma=(2\pi)^{-5}\frac{1}{2^5F}\frac{1}{4}\sum|M|^2\delta^4(p_1'+p_2'+q-p_1-p_2)\times\frac{d^3p_1'}{p_{10}'}\frac{d^3p_2'}{p_{20}'}\frac{d^3q}{q_0}, \qquad (4)$$

where F is the usual flux factor ($F=M_2p_1{}^L$) and the sum now runs over the spins of all baryons present. Transforming variables this becomes

$$d\sigma=(2\pi)^{-4}\frac{f_I}{2^7F^2}\frac{q^P}{u}\frac{1}{4}\sum|M|^2d\cos\theta^Pd\phi^Pdu^2dt, \qquad (5)$$

where $(\cos\theta^P,\phi^P)$ are angles defining the direction of emission of the pion, i.e., of $\mathbf{q}^P$, with respect to axes in the P frame chosen so that the z axis is in the direction of $\mathbf{p}_2{}^P$. A factor f_I has been inserted to allow for summation over different isotopic spin states within the P system. We wish to calculate $d^2\sigma/dudt$ but the remaining integration over $(\cos\theta^P,\phi^P)$ cannot be done until J and $\mathcal{P}$ analysis of M.

B. Angular Momentum and Parity Analysis

The model requires spin independence of the diffraction scattering process, which means that the sum and average over p_1', p_1 spins can be done independently. The amplitude for the *whole* process is therefore written, from (1) and (3),

$$M\equiv\langle\theta^P\phi^P\lambda_2'|S|00\lambda_2\rangle=i2\sqrt{2}q^Qwg^{1/2}(t)\sigma_{\rm tot}(\Delta^2+\mu^2)^{-1}M_2(\lambda_2',\lambda_2), \qquad (6)$$

where λ_2' and λ_2 are the helicities of p_2' and p_2. Note that M is a function of the angles (θ^P,ϕ^P) through $\Delta^2=-m_2{}^2-m_{2'}{}^2+2p_{20'}{}^Pp_{20}{}^P+2p_{2'}{}^Pp_2{}^P\cos\theta^P$ and of course the baryon-pion-baryon vertex $M_2(\lambda_2',\lambda_2)$. The whole process is thus equivalent to "scalar"$+p_2\to q+p_2'$, and the amplitude M may be resolved by usual methods[25] into final-state P systems of definite J. [This procedure may be *interpreted* as equivalent to assuming vacuon exchange, in which the vacuon has zero helicity, but any exchange mechanism which results in the whole process being independent of the spins of p_1 and p_1'

[24] The theoretical total cross section is twice the area under the curve of $d\sigma/dt$ since two diagrams contribute corresponding to the interchange of initial protons. There are two more diagrams which correspond to interchange of final nucleons and both initial and final nucleons together; these mean that the proton detected in a missing-mass spectrometer experiment comes from the dissociation vertex and so they are assumed to contribute to background only.

[25] M. Jacob and G. C. Wick, Ann. Phys. (N. Y.) 7, 404 (1959). References to equations in this paper are written as (JW-30), for example.

amounts to the same thing, and leads to the parity-change rule $\Delta P=(-1)^{\Delta L}$.]

Remembering that in the P frame p_2 is in the z direction and p_2' is in the direction (θ^P,ϕ^P), we have for that part of M leading to a P system in a particular state J (JW-30)

$$M_J\equiv\langle\theta^P\phi^P\lambda_2'|S^J|00\lambda_2\rangle$$
$$=(2\pi)^{-1}(J+\tfrac{1}{2})\langle\lambda_2'|S^J|\lambda_2\rangle e^{i(\lambda_2'-\lambda_2)\phi^P}d_{\lambda_2'\lambda_2}{}^J(\theta^P). \quad (7)$$

The matrix elements $\langle\lambda_2'|S^J|\lambda_2\rangle$ may then be combined to give amplitudes connecting states of definite $\mathcal{P}$, using the property (JW-43) describing their behavior under spatial reflections.

$$\begin{aligned}
&p_2'\text{ a }\tfrac{1}{2}^+\text{ baryon:}\quad \langle-\lambda_2'|S^J|-\lambda_2\rangle=-\langle\lambda_2'|S^J|\lambda_2\rangle\\
&\mathcal{P}=(-1)^{J+1/2},\quad U_J=\langle\tfrac{1}{2}|S^J|\tfrac{1}{2}\rangle+\langle-\tfrac{1}{2}|S^J|\tfrac{1}{2}\rangle \qquad (8a)\\
&\mathcal{P}=(-1)^{J-1/2},\quad u_J=\langle\tfrac{1}{2}|S^J|\tfrac{1}{2}\rangle-\langle-\tfrac{1}{2}|S^J|\tfrac{1}{2}\rangle\\
&p_2'\text{ a }\tfrac{3}{2}^+\text{ baryon:}\quad \langle-\lambda_2'|S_*{}^J|-\lambda_2\rangle=\langle\lambda_2'|S_*{}^J|\lambda_2\rangle\\
&\mathcal{P}=(-1)^{J+1/2},\quad U_J{}^*=\langle\tfrac{1}{2}|S_*{}^J|\tfrac{1}{2}\rangle-\langle\tfrac{1}{2}|S_*{}^J|-\tfrac{1}{2}\rangle\\
&\qquad\qquad V_J{}^*=\langle\tfrac{3}{2}|S_*{}^J|\tfrac{1}{2}\rangle-\langle\tfrac{3}{2}|S_*{}^J|-\tfrac{1}{2}\rangle \qquad (8b)\\
&\mathcal{P}=(-1)^{J-1/2},\quad u_J{}^*=\langle\tfrac{1}{2}|S_*{}^J|\tfrac{1}{2}\rangle+\langle\tfrac{1}{2}|S_*{}^J|-\tfrac{1}{2}\rangle\\
&\qquad\qquad v_J{}^*=\langle\tfrac{3}{2}|S_*{}^J|\tfrac{1}{2}\rangle+\langle\tfrac{3}{2}|S_*{}^J|-\tfrac{1}{2}\rangle.
\end{aligned}$$

The quantities relating to p_2' a $\frac{3}{2}^+$ baryon have now been labeled with an asterisk. Instead of Eq. (5), we may therefore write the partial differential cross section for the production of a spin-J P system,

$$\frac{d^2\sigma_J}{du^2dt}=(2\pi)^{-4}\frac{1}{2^7F^2}\frac{q^P}{u}\int\frac{1}{4}\sum_{\text{all spins}}|M_J|^2d\cos\theta^Pd\phi^P. \quad (9)$$

Using (7) one can perform this integration and summation over all baryon helicity states; e.g., in the case of p_2' a $\frac{1}{2}^+$ baryon,

$$\int\frac{1}{4}\sum_{\text{spins}}|M_J|^2d\cos\theta^Pd\phi^P=(8\pi)^{-1}(J+\tfrac{1}{2})\{|\langle\tfrac{1}{2}|S^J|\tfrac{1}{2}\rangle|^2$$
$$+|\langle\tfrac{1}{2}|S^J|-\tfrac{1}{2}\rangle|^2+|\langle-\tfrac{1}{2}|S^J|\tfrac{1}{2}\rangle|^2+|\langle-\tfrac{1}{2}|S^J|-\tfrac{1}{2}\rangle|^2\}$$
$$=(8\pi)^{-1}(J+\tfrac{1}{2})\{\tfrac{1}{2}|u_J+U_J|^2+\tfrac{1}{2}|u_J-U_J|^2\},$$

using (8a). Because these amplitudes are pure imaginary, there is no interference between states of different parity. The partial cross sections for producing a spin-J state of parity $(-1)^{J\pm1/2}$ are therefore

$$\mathcal{P}=(-1)^{J\pm1/2}:\quad\frac{d^2\sigma_{J\pm}}{dudt}=(2\pi)^{-5}\frac{f_I}{2^8F^2}q^P(J+\tfrac{1}{2})\begin{pmatrix}|U_J|^2\\|u_J|^2\end{pmatrix} \quad (10a)$$

and

$$\mathcal{P}=(-1)^{J\pm1/2}:\quad\frac{d^2\sigma_{J\pm}{}^*}{dudt}=(2\pi)^{-5}\frac{f_I{}^*}{2^8F^2}q^P(J+\tfrac{1}{2})\times\begin{pmatrix}|U_J{}^*|^2+|V_J{}^*|^2\\|u_J{}^*|^2+|v_J{}^*|^2\end{pmatrix}. \quad (10b)$$

Note that in our model interferences between states of different J do not affect (9) because of the orthogonality property of the d^J's. However, one might expect interference with other diagrams than that of Fig. 2(a).

The amplitudes u_J, etc., have to be calculated in terms of the helicity amplitudes $\langle\lambda_2'|S^J|\lambda_2\rangle$ or $\langle\lambda_2'|S_*{}^J|\lambda_2\rangle$ for the $\frac{1}{2}^+\to0^-+(\frac{1}{2}^+\text{ or }\frac{3}{2}^+)$ vertices. The latter can be obtained from our original amplitude (6) by using the inverse of (7), namely,

$$\langle\lambda_2'|S^J|\lambda_2\rangle=\int_{-1}^{1}d\cos\theta^P\int_0^{2\pi}d\phi^P\langle\theta^P\phi^P\lambda_2'|S|00\lambda_2\rangle$$
$$\times d_{\lambda_2'\lambda_2}{}^J(\theta^P)e^{i(\lambda_2-\lambda_2')\phi^P}. \quad (11)$$

The helicity amplitudes $M_2(\lambda_2',\lambda_2)$ have been calculated by Frishman and Gotsman.[26] After simplification of the resulting expressions one obtains finally

p_2' a $\frac{1}{2}^+$ baryon:

$$\begin{pmatrix}U_J\\u_J\end{pmatrix}=i4\pi\sqrt{2}\sigma_{\text{tot}}q^{1/2}(t)G\int_{-1}^{1}dz$$
$$\times[J_+J_-'P_{J\pm1/2}(z)-J_-J_+'P_{J\mp1/2}(z)]$$
$$\times(\Delta^2+\mu^2)^{-1}\bar{h}(z), \quad (12)$$

where

$$J_\pm=(p_{20}{}^P\pm m_2)^{1/2},\quad J_\pm'=(p_{20'}{}^P\pm m_2')^{1/2},\quad z=-\cos\theta^P,$$

and

$$\bar{h}(z)=\frac{1}{4\pi}\int_0^{2\pi}(w^2-m_1{}'^2)d\phi^P$$
$$=\tfrac{1}{2}m^2+p_{10'}{}^Pq_0{}^P+p_{1'}{}^Pq^P\cos\chi^Pz. \quad (13)$$

Here χ^P is the angle of $\mathbf{p}_{1'}{}^P$ to the z axis, given by

$$\cos\chi^P=[p_{20}{}^P(p_{10'}{}^P+u)$$
$$-\tfrac{1}{2}(u^2+m_2{}^2-m_1{}^2+m_1{}'^2+2up_{10'}{}^P)]/p_2{}^Pp_{1'}{}^P, \quad (14)$$

a fixed quantity for u^2, t fixed.

A result equivalent to (10a) with (12) has been obtained previously by Resnick.[11]

---

[26] Y. Frishman and E. Gotsman, Phys. Rev. **140**, B1152 (1965). For calculational convenience these authors chose a set of axes in which the outgoing baryon is along the z axis, different from our scattering geometry. The integral (11) has been transformed to allow for this in arriving at the results (12)–(16).

p_2' a $\frac{3}{2}^+$ baryon:

$$\begin{pmatrix} U_J^* \\ u_J^* \end{pmatrix} = i4\pi\sqrt{2}\sigma_{\text{tot}} g^{1/2}(t)\left(-\frac{G^*}{\mu}\right)\int_{-1}^{1} dz \frac{1}{\sqrt{6}}(\Delta^2+\mu^2)^{-1}\bar{h}(z) J_+ J_+' \times \left\{\left[\left(\frac{2p_{20}{}^P p_{2'}{}^P}{m_2'}+\frac{(p_2{}^P)^2 p_{2'}{}^P}{(J_+)^2(J_+')^2}\right)-\left(p_2{}^P+\frac{2p_2{}^P p_{20'}{}^P}{m_2'}\right)z\right]P_{J\pm 1/2}(z) + \left[\left(p_2{}^P-\frac{2p_{20}{}^P p_2{}^P (p_{2'}{}^P)^2}{m_2'(J_+)^2(J_+')^2}\right)+\left(-p_2{}^P+\frac{2p_2{}^P p_{20'}{}^P}{m_2'}\right)\frac{p_2{}^P p_{2'}{}^P}{(J_+)^2(J_+')^2}z\right]P_{J\pm 1/2}(z)\right\} \quad (15)$$

and

$$\begin{pmatrix} V_J^* \\ v_J^* \end{pmatrix} = i4\pi\sqrt{2}\sigma_{\text{tot}} g^{1/2}(t)\left(-\frac{G^*}{\mu}\right)\int_{-1}^{1} dz \frac{1}{\sqrt{2}}(\Delta^2+\mu^2)^{-1}\bar{h}(z)\frac{[(J-\frac{1}{2})(J+\frac{3}{2})]^{1/2}}{(J+\frac{1}{2})} \times (\pm p_2{}^P) J_+ J_+' \left[\frac{p_2{}^P p_{2'}{}^P}{(J_+)^2(J_+')^2}P_{J\mp 3/2}(z)+P_{J\pm 3/2}(z)-\frac{p_2{}^P p_{2'}{}^P}{(J_+)^2(J_+')^2}zP_{J\mp 1/2}(z)-zP_{J\pm 1/2}(z)\right]. \quad (16)$$

The isospin factors f_I, $f_I{}^*$ will be determined after the inclusion of the final-state resonant interaction. In the usual way Eqs. (10a) and (10b) must be multiplied by 2.57 to obtain mb $(\text{GeV})^{-1}$ $(\text{GeV}/c)^{-2}$ when all dynamical quantities are in GeV. The value 28 mb has been used for σ_{tot}, and the diffraction shape taken as $g(t) = \exp(-bt+ct^2)$ with $b=9$, $c=2.5$ from experimental data.[27]

Figures 3(a) and 3(b) show typical spectra calculated from Eqs. (10a) and (10b) for $pp \to pN\pi$ and $pp \to p\Delta\pi$ for a number of $J^{\mathcal{P}}$ values, corresponding to natural parity (full curves) and "unnatural" parity (dashed curves) states. These give $d^2\sigma/dudt$ versus u calculated at the particular value $t=0.1$ $(\text{GeV}/c)^2$. As indicated in Sec. II A, states with $J=\frac{1}{2}$ dominate for (10a) and states with $J=\frac{1}{2}, \frac{3}{2}$ dominate for (10b); this is evidently due to the presence of $P_0(z)$ in Eqs. (12), (15), and (16).

As a numerical check on the above calculations, instead of a spin-parity analysis of M we can perform a trace calculation in (5) to obtain directly

$$\frac{d^2\sigma}{dudt} = (2\pi)^{-2}\frac{\sigma_{\text{tot}}{}^2}{2^4F^2}q^P g(t)\int_{-1}^{1}(\Delta^2+\mu^2)^{-2}h(z)G(z)dz, \quad (17)$$

where, with p_2' a $\frac{1}{2}^+$ baryon,

$$G(z) = f_I(G^2/4\pi)2[(m_2-m_2')^2+\Delta^2], \quad (18a)$$

and with p_2' a $\frac{3}{2}^+$ baryon,

$$G(z) = f_I{}^*(G^{*2}/4\pi)(3\mu^2 m_2'^2)^{-1} \times [(m_2-m_2')^2+\Delta^2]^2[(m_2+m_2')^2+\Delta^2], \quad (18b)$$

and where

$$h(z) = (q_0{}^P p_{10'}{}^P + z p_{1'}{}^P q^P \cos\chi^P)^2 + \tfrac{1}{2}(p_{1'}{}^P q^P \sin\chi^P)^2(1-z^2). \quad (19)$$

[27] K. J. Foley *et al.*, Phys. Rev. Letters **11**, 425 (1963); D. Harting *et al.*, Nuovo Cimento **38**, 60 (1965).

It is clear that (10) and (17) are related by

$$d\sigma = \sum_J (d\sigma_{J+}+d\sigma_{J-}) \quad (20)$$

and the curves shown in Figs. 3(a) and 3(b) labelled "all $J^{\mathcal{P}}$" calculated from (17) show that this is satisfied.

C. Final-State Resonant Interaction

The exact calculation of Fig. 2(b) requires the evaluation of a triangle diagram and would raise problems beyond the scope of this paper. Watson[28] has given an expression for the effect of final-state interactions on reaction cross sections which requires that the final-state force be much stronger than the production process and take place attractively between only one pair of particles. Delbourgo[29] has considered the more general case where the final-state interactions and the production process are of comparable strength, as is the case here. A covariant calculation leads to the following intuitively reasonable result: If the final-state interaction occurs in a particular state J of the interacting pair q and p_2', is independent of helicities, and is measured by the phase shift δ_J, then the production amplitude after including the final-state interaction is obtained from the original amplitude M_J by the replacement

$$M_J \to M_J\left(1+c_J\frac{e^{i\delta_J}\sin\delta_J}{2q^P/u}\right). \quad (21)$$

Here c_J provides a measure of the amount of final-state scattering that takes place and can be shown to be ≈ 1. This formula requires that only the lowest order in the final-state scattering channel be retained. For the purposes of this calculation we shall take $c=1$.

[28] K. M. Watson, Phys. Rev. **88**, 1163 (1952).
[29] R. Delbourgo, Nucl Phys. **38**, 281 (1962).

The formula is to be interpreted in this context in the following way. As well as the original amplitude M_J producing the smooth, nonresonating background of Figs. 3(a) and 3(b), there appears the same amplitude modulated to allow for final-state scattering. Therefore $d^2\sigma/dudt$ carries, in addition to the original Drell-Hiida background expressed by (10a) and (10b), a distribution given by

$$(d^2\sigma/dudt)\times c_J{}^2(u/2q^P)^2\sin^2\delta_J.$$

On taking a resonant-phase shift approximation[30] to δ_J and allowing for the input and output channels considered, we have finally as an estimate of the differential cross section for producing a given resonance:

$$\left(\frac{d\sigma}{dt}\right)_{\rm res}=\int_{u_0-\Gamma}^{u_0+\Gamma}c_J{}^2\left(\frac{u}{2q^P}\right)^2 \times\frac{u_0{}^2\Gamma_{\rm in}\Gamma_{\rm tot}(u)}{(u_0{}^2-u^2)^2+u_0{}^2\Gamma_{\rm tot}{}^2(u)}\frac{d^2\sigma}{dudt}du. \quad (22)$$

Here u_0 is the mass of the appropriate resonance, $\Gamma_{\rm in}$ is the partial width for the input channel, and $\Gamma_{\rm tot}$ the total width in the exit channel for the final-state interaction $\pi+(N$ or $\Delta)\rightarrow N_{1/2}{}^*\rightarrow$ all channels. The usual

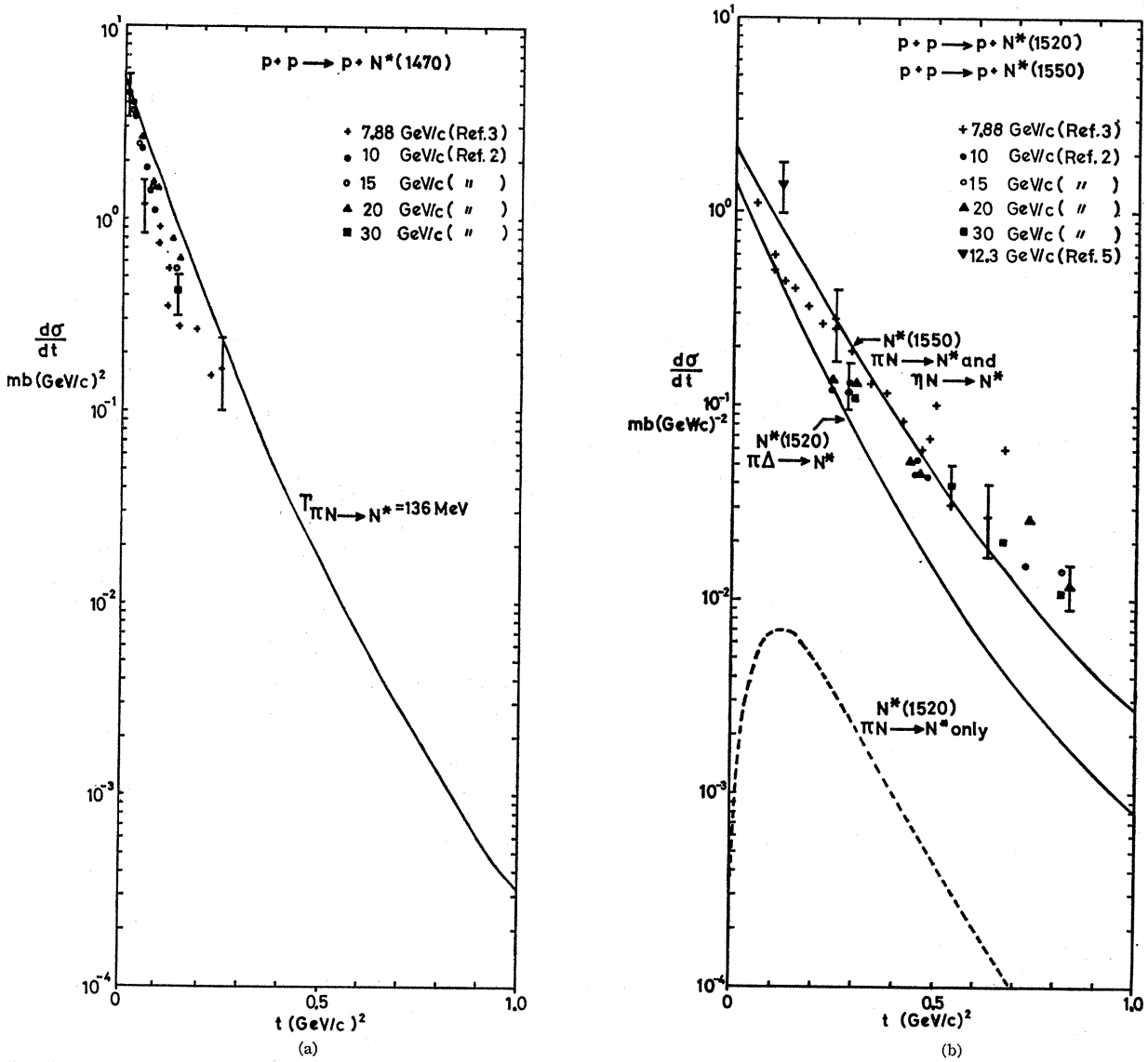

FIG. 4. Comparison of model with experimental differential cross section $d\sigma/dt$ for process $pp\rightarrow pN_{1/2}{}^*$ for the resonances (a) $P_{11}(1470)$, (b) $D_{13}(1520)$ and $S_{11}(1550)$, (c) $F_{15}(1690)$ and $P_{11}(1750)$, (d) $G_{17}(2190)$ and $D_{13}(2030)$. Resonance paameters as in Table I and as indicated. Experimental errors are in the range 25–50%.

[30] J. D. Jackson, Nuovo Cimento 34, 1644 (1964).

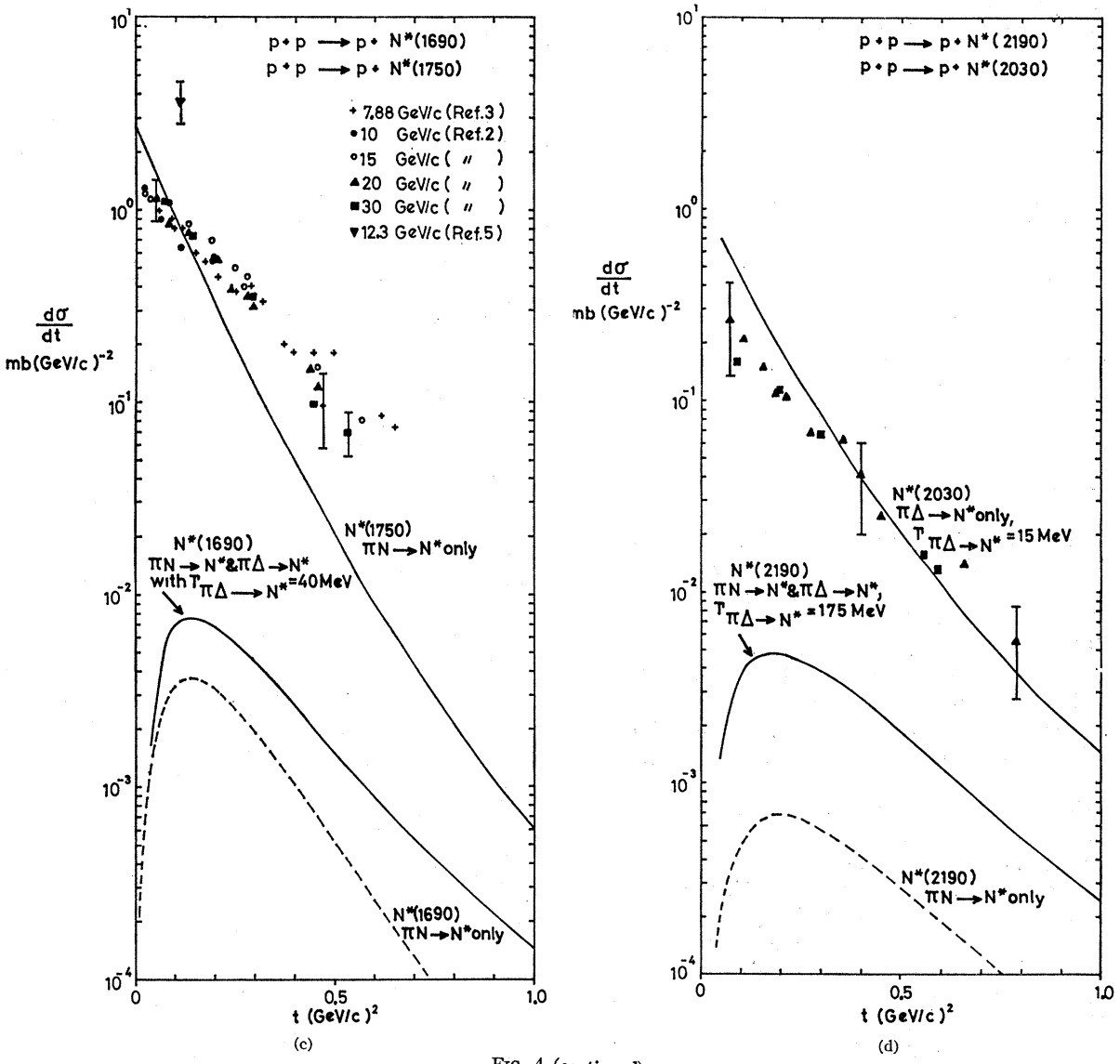

FIG. 4 (*continued*)

expression for a mass-dependent width

$$\Gamma(u)=\Gamma_0(q^P/q_0^P)^{2l+1}$$

is used.

There will also be interference between the two parts of (21); as M_J is pure imaginary, this will be zero at $u=u_0$ [as it is proportional to $(u_0^2-u^2)$], and we assume will be taken as contributing to background. In keeping with the spirit of this calculation we assume that all other final-state effects and interferences lead to a relatively smooth background in u from which the resonant contribution (22) can be distinguished (and hopefully *has* been distinguished in interpreting experimental spectra).

Finally we have to evaluate f_I and f_I^*. For f_I there are two diagrams: π^+ scattering with a factor $(\sqrt{2}G\times\sqrt{\frac{2}{3}})^2$ coming from dissociation and resonance vertices, and π^0 scattering with a corresponding factor $(G\times\sqrt{\frac{1}{3}})^2$; hence $f_I=5/3$. For f_I^* there are three diagrams, incorporating π^-, π^0, and π^+ scattering; these give in turn $(G^*\times\sqrt{\frac{1}{2}})^2+[(\sqrt{\frac{2}{3}})G^*\times\sqrt{\frac{1}{3}}]^2+[(\sqrt{\frac{1}{3}})G^*\times\sqrt{\frac{1}{6}}]^2$, and hence $f_I^*=7/9$ (recalling that G^* refers to the $p\to\pi^-\Delta^{++}$ vertex).

III. RESULTS AND COMPARISON WITH EXPERIMENT

Table I lists the current position[23] concerning $I=\frac{1}{2}$ nucleon resonances resulting from πN phase-shift analyses. In the light of this list it is very probable that some of the enhancements identified by missing-mass experimenters[1–5] are in fact composites of more than one of these resonances, particularly in view of their large widths. Any detailed fit to the data would there-

TABLE I. Resonances observed[a] in pion-nucleon scattering phase-shift analyses. The first six are definite and appear in the Particle Data Group list,[b] the last six are uncertain. The values quoted for $\Gamma_{N^*\to\Delta\pi}$ are very tentative only. (All masses in MeV.)

Resonance	$J^{\mathcal{P}}$	Γ_{tot}	$\Gamma_{N^*\to N\pi}$	$\Gamma_{N^*\to\Delta\pi}$
$P_{11}(1470)$	$\frac{1}{2}^+$	210	136	~ 20
$D_{13}(1520)$	$\frac{3}{2}^-$	115	63	~ 14
$S_{11}(1550)$	$\frac{1}{2}^-$	130	39	$(\Gamma_{N^*\to N\eta}=9)$
$D_{15}(1680)$	$\frac{5}{2}^-$	170	68	~ 25
$F_{15}(1690)$	$\frac{5}{2}^+$	130	84	~ 25
$S_{11}(1710)$	$\frac{1}{2}^-$	300	240	
$D_{13}(1730)$	$\frac{3}{2}^-$	?	?	
$P_{11}(1750)$	$\frac{1}{2}^+$	327	105	
$P_{13}(1860)$	$\frac{3}{2}^+$	296	61	
$F_{17}(1980)$	$\frac{7}{2}^+$	225	29	
$D_{13}(2030)$	$\frac{3}{2}^-$	290	76	
$G_{17}(2190)$	$\frac{7}{2}^-$	300	115	

[a] Reference 23.
[b] Reference 22.

fore be premature, and the model described above will be discussed only in relation to the broad features observed, which might be summarized as follows: (i) At the low-mass end of the spectrum the $P_{11}(1470)$ and $D_{13}(1520)$ are often resolved on the basis of their different t dependences, the $P_{11}(1470)$ being characterized by a steep slope in t [$\sim$15–20 $(\text{GeV}/c)^{-2}$], as compared with about 4–5 $(\text{GeV}/c)^{-2}$ for all other $N_{1/2}{}^*$'s. (ii) The enhancement centered at about 1700 MeV, possibly involving as many as five resonances. (ii) The highest-mass enhancement, previously identified with the $G_{17}(2190)$.

It is apparent from Fig. 3(a) that S_{11} and P_{11} states are favored by having p_2' a nucleon, whilst D_{13} and P_{11} states can be strongly produced if p_2' is a $\Delta(1236)$ as indicated in Fig. 3(b) [where natural parity states are seen to be favored over the unnatural parity states of the same J]. As S_{11} and P_{11} states with mass near 1700 MeV appear in Table I, the model suggests that it could be these states rather than the $F_{15}(1690)$ which is being observed. Similarly it could be the $D_{13}(2057)$ rather than the $G_{17}(2190)$, provided there proves to be a substantial partial width $\Gamma_{N^*\to\Delta\pi}$ for the D_{13} resonance. (It should be remembered[23] that resonance positions obtained from a variety of phase-shift analyses can differ by typically 10–20 MeV and up to 100 MeV in one or two cases. Positions of experimental enhancements are also subject to background assumptions.)

We shall now examine some numerical predictions of the model for the above features using $(d\sigma/dt)_{\text{res}}$ from Eq. (22) and the resonance parameters of Table I. Spectra in t for some of the resonances are given in Figs. 4(a)–4(d) and compared with available experimental data. Absolute errors on data points are typically 25–50%. All curves shown are calculated for $p_1{}^L=20$ GeV/c, being only slightly dependent on $p_1{}^L$.

(i) In the case of the $P_{11}(1470)$ the theoretical contribution comes predominantly from the πN resonant channel and gives about the right magnitude and slope [$b\sim 13$ $(\text{GeV}/c)^{-2}$]. Figure 5 shows a favorable comparison between theoretical[24] and experimental[2,3] total cross sections for the $P_{11}(1470)$ over the laboratory momentum range 10–30 GeV/c. The exact position of the $N^*(1470)$ resonance is itself in some doubt. Counter experimenters seem to agree that the bump at low t values is centered at about 1410 MeV, while at higher t values it merges with the $N^*(1525)$. Bubble-chamber experimenters,[18] on the other hand, usually observe a peak nearer the phase-shift value of 1470 MeV, which has been used in this calculation. Use of the lower mass reduces the differential and total cross sections by about 15%.

For the $D_{13}(1520)$ the $\pi\Delta$ channel is found to make the dominant contribution. Using the tentative value $\Gamma_{\pi\Delta\to N^*}=14$ MeV the curve shown in Fig. 4(b) is obtained, which falls below the experimental points and has too steep a slope. A feature of the model is that the slope in t is a decreasing function of the mass, which is an observed property[31] of the diffraction dissociation process. The slope is also steepest for systems of low spin ($J=\frac{1}{2}, \frac{3}{2}$).

(ii) Turning to the 1700-MeV enhancement [see Fig. 4(c)], the model predicts far too little cross section for the $F_{15}(1690)$ even if the whole inelastic channel were $\pi\Delta\to N^*$. However, as pointed out above, there are many resonances which might be involved in this mass region, e.g., taking the $P_{11}(1750)$, the model predicts a $d\sigma/dt$ of about the right magnitude but with too steep a slope. The model has no interferences between states of different J or $\mathcal{P}$, and fortunately no two resonances in the 1700-MeV region have the same J and $\mathcal{P}$.

(iii) Considering the high-mass region [Fig. 4(d)], the data cannot be matched on the assumption that the $G_{17}(2190)$ is being observed. The $D_{13}(2057)$ is not known to have a $\pi\Delta$ decay channel, but if only $\sim$7% of the inelastic channel were in this mode ($\Gamma_{\pi\Delta\to N^*}=15$ MeV) the data are seen to be roughly accounted for.

A variety of form factors in Δ^2 were introduced into (12), (15), and (16) which had the effect of altering $(d\sigma/dt)_{\text{res}}$ in absolute magnitude, leaving slopes in t unaffected.

Finally, the model makes no distinction between natural and unnatural parity resonances in the absence of a deeper understanding of the mechanism of Pomeranchukon exchange. However, as far as experimental evidence goes, there appears to be little to suggest that unnatural parity resonance production is being suppressed. The nonappearance of the $S_{11}(1550)$ has been singled out[8] as possible evidence in support of the natural parity selection rule. It is therefore interesting to see what the model predicts for this resonance. In calculating η exchange a value $g_{NN\eta}{}^2/4\pi=2$ was taken

[31] W. D. Walker *et al.*, Phys. Rev. Letters **20**, 133 (1968).

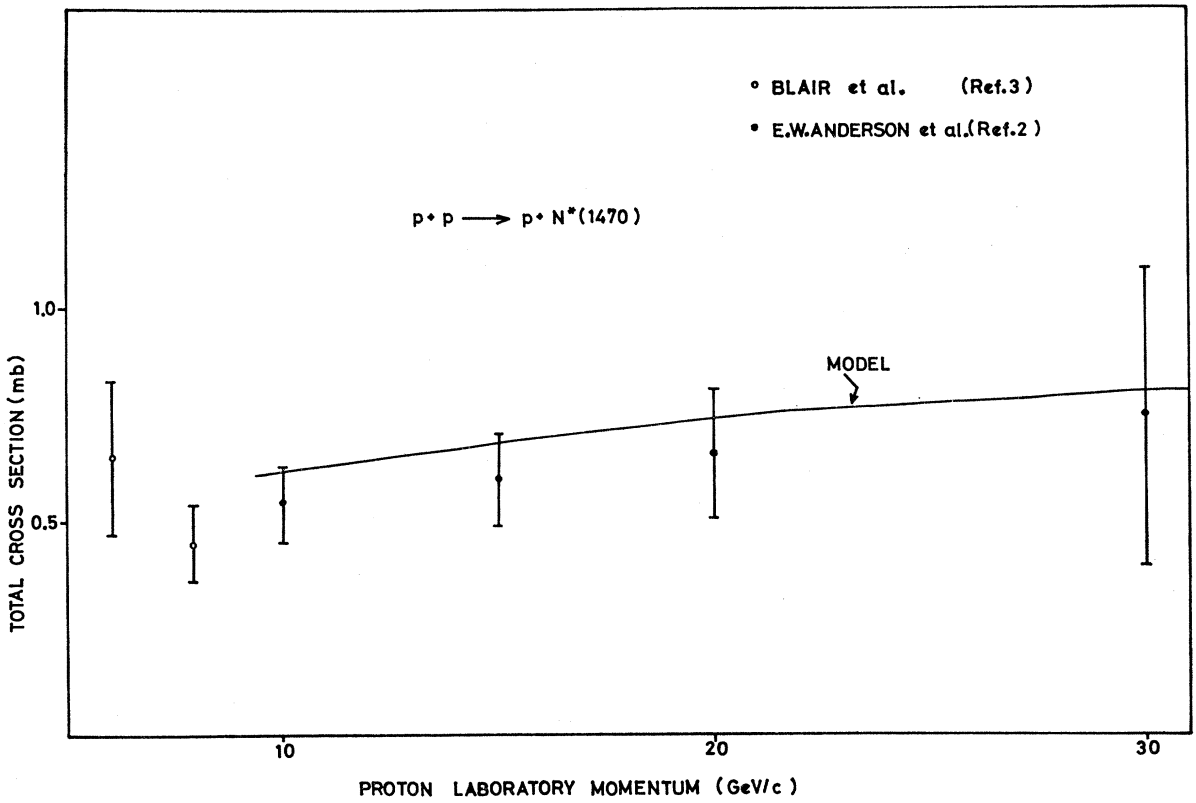

FIG. 5. Total cross section for $pp \rightarrow pN^*(1470)$. Comparison of model prediction and experimental values.

as the suggested[32] maximum value of this coupling constant, and the η-exchange contribution was found to be about one-third of that from π exchange. Adding these contributions, the differential cross section for producing the $S_{11}(1550)$ is thereby shown [Fig. 4(b)] to be larger than that for the $D_{13}(1525)$, and in quite reasonable agreement with the data. It is therefore tempting to speculate that there is no natural parity rule, and it is mostly the $S_{11}(1550)$ being observed (phase-shift analysts put its mass as low as 1499 MeV).

IV. CONCLUSIONS

A model akin to the diffraction dissociation process has been described for reactions $pp \rightarrow pN_{1/2}^*$ incorporating one-meson exchange with final-state resonant interaction. Absolute calculations of differential and total cross sections have been made. Total cross sections are found to be fairly constant with energy. These predictions agree quite favorably with experiment in the case of the $P_{11}(1470)$. In higher-mass regions much more accurate experimental data is needed to resolve the many $N_{1/2}^*$'s obtained by phase-shift analyses before the model can be adequately tested.

The model is neutral with regard to the suggested $\Delta P = (-1)^{\Delta J}$ selection rule and predicts a large cross section for the forbidden $S_{11}(1550)$.

Desirable refinements of the model would include consideration of off-shell effects with the final-state resonant interaction, and Reggeization of the exchanged pion. Other limiting assumptions in the model have been discussed in the introduction.

Finally, these calculations suggest a possible means of estimating that resonant amplitude which Chew and Pignotti have pointed out is contained within the Drell-Hiida (or Deck) background. A partial-wave decomposition of the resonating system can be performed in the model, leading to the curves of Figs. 3(a) and 3(b). We therefore suggest that double-counting of a resonance could be avoided by subtracting the appropriate partial wave from the full Deck amplitude (labelled "all $J^{\mathcal{P}}$") before adding in any "genuine" resonant amplitude in seeking to match experimental mass distributions.

ACKNOWLEDGMENT

The author is grateful to the Institute of Theoretical Astronomy in Cambridge for the use of their IBM 360/44 computer.

[32] S. R. Deans and W. G. Holladay, Phys. Rev. **161**, 1466 (1967).